Turk J Phys
31 (2007) , 279 – 286.

Thickness Dependent Structural, Electrical and Optical Properties of Chemically Deposited Nanopartical PbS Thin Films

A. U. UBALE, A. R. JUNGHARE, N. A. WADIBHASME, A. S. DARYAPURKAR, R. B. MANKAR, V. S. SANGAWAR

Thin Film Physics Laboratory, Department of Physics, Govt. Vidarbha Institute of Science and Humanities, Amravati, 444 604-INDIA

e-mail: ashokuu@yahoo.com

Received 10.05.2007

Abstract

Nanostructured thin films have attracted the attention of an increasing number of researchers from several disciplines during the last ten years, due to their outstanding electronic and optical properties and extensively useful applications in various optoelectronic devices. PbS thin films were deposited onto glass substrate by the method of chemical bath deposition (CBD) at 330 K temperature. The structure and surface morphology of the films were characterized by X-ray diffraction and scanning electron microscopy. The optical investigation showed that, depending on thickness films have direct allowed transitions in the range 1.88–2.28 eV. The decrease in dc dark resistivity with increase in grain size was also studied. The thermo-emf measurements show that deposited films were p-type in nature.

Key Words: Thin film, PbS, CBD method, electrical and optical properties.

1. Introduction

In recent years there has been increasing interest in the size-dependent electrical and optical properties of semiconductors [1–3]. In nanocrystallites, the electrons confined in a narrow potential well exhibit extraordinary characteristics in the optical and electrical properties [4]. When the width of such confining potential is very small i.e. of the order of few hundred angstroms, quantum size effect arises [5]. During the last few years, the research on the growth of nanoparticle PbS films has increased, for its technological applications in photoresistance, diode lasers, decorative coatings, and optoelectronic devices [6–12]. Many researchers have reported properties of chemically deposited PbS thin films [13–17]. The method of chemical bath deposition (CBD) is based on successive adsorption and reaction of species on the substrate surface from aqueous solutions. It does not require sophisticated and expensive instruments. By CBD method pinhole-free thin films have been grown easily since the basic building blocks are ions instead of atoms. In this paper, we present the synthesis of nanocrystalline PbS thin films using CBD method. Preparative parameters such as concentration of $Pb^{2+}$and S^{2-} ions, temperature and pH were optimized to obtain good quality of PbS thin films on glass. The size dependent properties of films were studied by X-ray diffraction, optical absorption, and electric and thermo-emf measurements.

2. Experimental Details

The important thing before the deposition of films is the careful cleaning of the substrates. As the cleanliness of the substrate has a direct bearing on the adherence of the film, the following procedure was adopted for cleaning the substrates. The slides were washed with liquid detergent and then boiled in concentrated chromic acid (0.5 M) for 2 hours, after which the slides were kept in this for a further 48 hours. The substrates were then washed with double distilled water. Finally, the substrates were dried using AR grade acetone before use. For deposition of PbS thin films, lead acetate was used as Pb^{2+} and thiourea as S^{2-} source in an alkaline medium. For this, 45 ml solutions of 0.05 M lead acetate, and 0.05 M thiourea were mixed together. The pH of the bath was adjusted to 10 by drop-wise addition of ammonia. The mixture was heated at 330 K temperature for 10 minutes, then kept at room temperature for further deposition. The average thickness of the film was measured by the gravimetric and Fizzau's method. The two-point dc probe method of dark electrical resistivity was used to study the variation of resistivity with temperature. A copper block was used as a sample holder and chromel-alumel (type K) thermocouple was used to measure the temperature. The area of the film (0.5 cm^2) was defined and silver paste was applied to ensure good ohmic contact to PbS films. For the measurement of resistivity, a constant voltage was applied across the sample and the current was noted using a digital nanoammeter. Structural studies were carried out using Philips PW 1710 diffractometer, with Cu-Ka radiation having wavelength $\lambda = 1.5405$ Å. The optical characteristics were studied using Hitachi 330 spectrophotometer to find band gap energy. Microstructural was studied using JSM-6360 scanning electron microscope.

3. Results and Discussion

3.1. Reaction mechanism

The CBD is based on sequential reaction at the substrate surface. The formation of PbS may involve the following steps. In an aqueous solution lead acetate releases Pb^{2+} ions as

$$Pb(CH_3COO)_2 \rightarrow Pb^{2+} + 2CH_3COO^- \tag{1}$$

In alkaline medium, dissociation of $(NH_2)_2CS$ takes place,

$$\begin{array}{l} \quad\quad S \\ \quad\quad || \\ NH_2- \; C = NH_2 + OH^- \rightarrow CH_2N_2 + H_2O + SH^- \end{array} \tag{2}$$

$$SH^- + OH^- \rightarrow S^{2-} + H_2O \tag{3}$$

$$Pb^{2+} + S^{2-} \rightarrow PbS \downarrow \tag{4}$$

The reaction solution colour changed to brownish black after heating for ten minutes, indicating initiation of chemical reaction. At the end of different duration of depositions, the substrates coated on both sides with blackish films, were removed from the bath, washed well with de-ionized water and dried. The PbS thin film deposited on the side of the substrate facing the beaker wall was retained for all analysis. The coating on the outer side was removed with dilute acid and preserved in airtight chamber.

Using optimized conditions and by changing deposition time period the films having thickness 65 to 168 nm was prepared (Figure 1). Films prepared by chemical bath deposition method were uniform, adherent to substrates and blackish in colour.

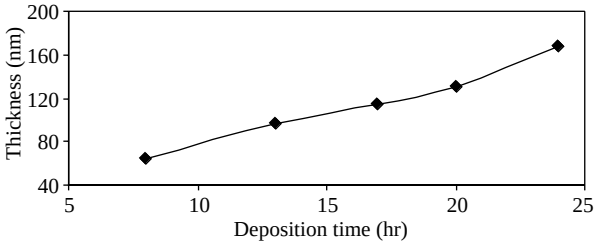

Figure 1. Variation of PbS film thickness with number of deposition cycles.

3.2. XRD studies

Structural identification of PbS films was carried out with X-ray diffraction in the range of angle 2θ between 10° to 100°. Figure 2 shows the XRD patterns for PbS thin films, which were nanocrystalline in nature. The observed broad hump in XRD pattern is due to amorphous glass substrate. The comparison of XRD data with standard ASTM data (JCPDS card 5-592) is given in Table, which confirms cubic phase (galena) of PbS. The well defined (111), (200), (220), and (311) peaks were observed in the XRD patterns.

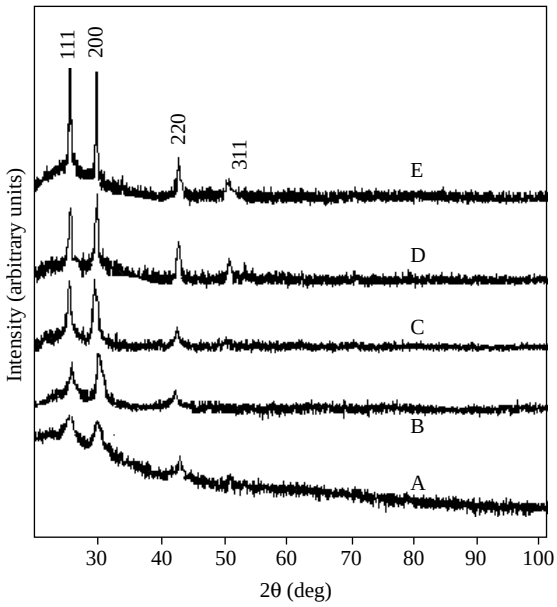

Figure 2. X-Ray diffraction patterns of PbS thin film of different thicknesses: (A) 65 nm, (B) 98 nm, (C) 114 nm, (D) 130 nm and (E) 168 nm.

Table. Comparison of crystallographic data for PbS thin films with the JCPDS card 5-592.

Standard data			Observed d values for PbS film (Å)			
d (Å)	hkl	Thickness 65 nm	Thickness 98 nm	Thickness 114 nm	Thickness 130 nm	Thickness 168 nm
3.429	111	3.430	3.431	3.428	3.430	3.428
2.969	200	2.971	2.974	2.966	2.970	2.971
2.099	220	2.101	2.102	2.103	2.101	2.095
1.790	311	-	-	1.790	1.792	1.789

The average crystallite size of PbS in the film was determined from the line (200) by using Scherrer formula

$$d = \frac{0.9\lambda}{\beta\cos\theta}, \tag{5}$$

where λ is the wavelength used (0.154 nm), β is the angular line width at half maximum intensity, and θ is the Bragg angle. Figure 3 shows variation of grain size from 13–35 nm with film thickness, which shows that the crystallinity of PbS increases with thickness.

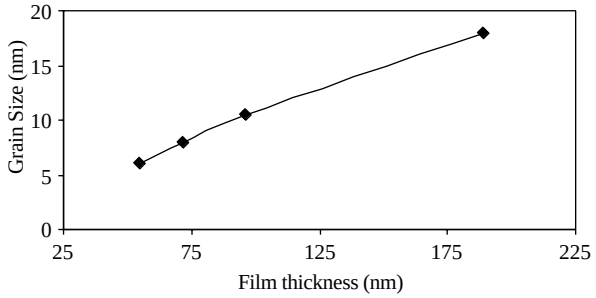

Figure 3. Variation of grain size with film thickness of PbS.

3.3. Resistivity studies

The dark electrical resistivity of PbS films was studied in the temperature range 303 to 480 K using dc two-point probe method. Figure 4 shows the variation of log of resistivity (log ρ) with reciprocal of temperature, $(1/T) \times 10^3$. It is seen that resistivity decreases with temperature, indicating semiconducting nature of films.

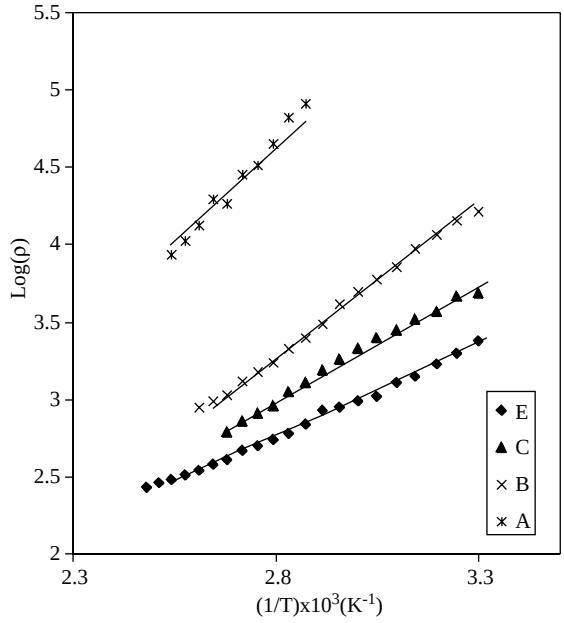

Figure 4. Variation of $\log(\rho)$ as a function of $1/T \times 10^3$ (K^{-1}) for PbS films with different thicknesses: (A) 65 nm, (B) 98 nm, (C) 114 nm, (D) 130 nm and (E) 168 nm.

The thermal activation energy was calculated using the relation

$$\rho = \rho_0 \exp(E_0/KT) \tag{6}$$

where, ρ is resistivity at temperature T, ρ_0 is a constant, K is Boltzmann constant

(8.62×10^{-5} eV/K) and E_0 is the activation energy required for conduction. Figure 5 shows variation in activation energy from 0.64 to 0.11 eV as thickness changes from 65 to 168 nm. These observations may be due to size effects that are arising because of quantum confinement of charge carriers within the particles. The thermally generated voltage at the cold end is positive, indicating the films are of p-type. Increase in thermo-emf with increasing film thickness (Figure 6) is attributed to the decrease in electrical resistivity caused by increase in grain size.

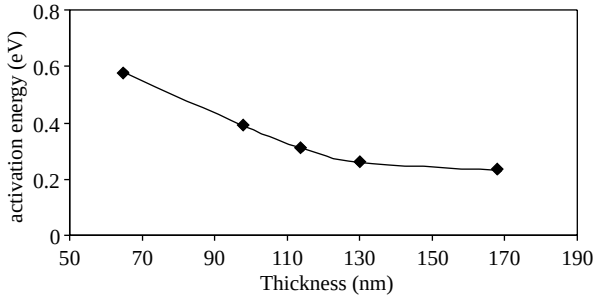

Figure 5. Variation of activation energy of PbS with film thickness

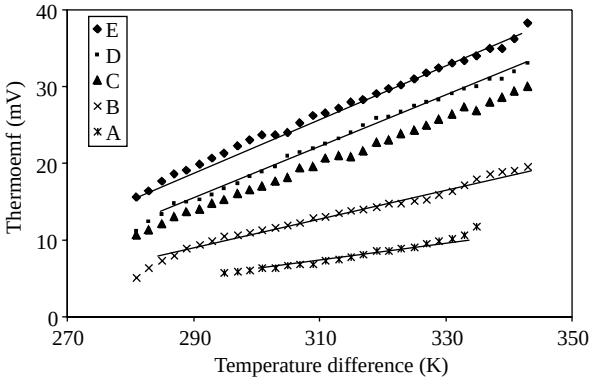

Figure 6. Variation of thermo-emf and temperature difference of PbS film with different thicknesses: (A) 65 nm, (B) 98 nm, (C) 114 nm, (D) 130 nm and (E) 168 nm.

3.4. SEM studies

The morphology of PbS thin films of thickness 65, and 168 nm deposited on glass substrate was examined by scanning electron microscopy (SEM) (Figure 7). The surface of the film is smooth and covers to the glass substrate well. The grains are very small with unequal size and shape.

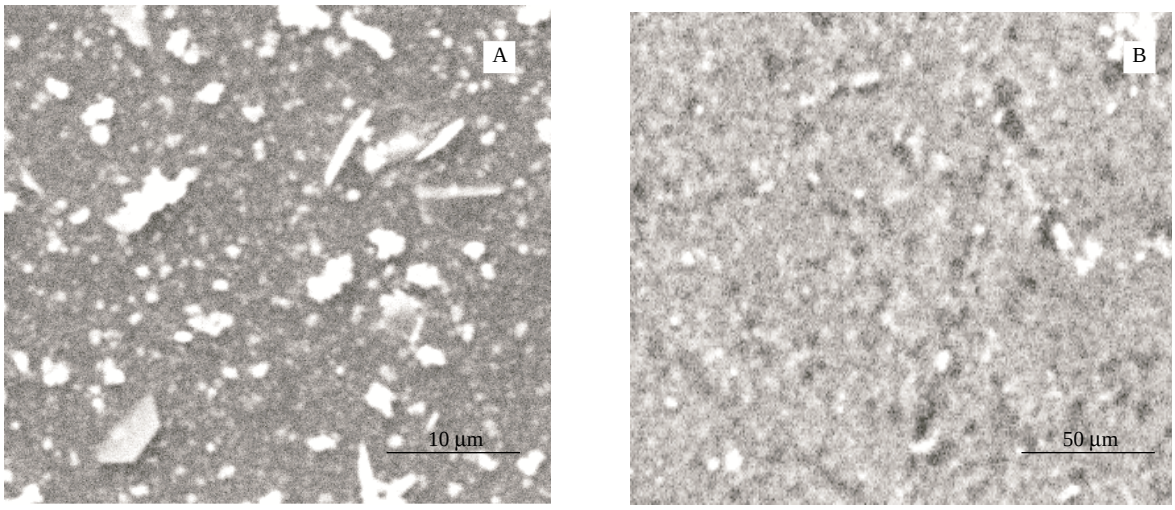

Figure 7. SEM images of PbS film of thicknesses 65 and 168 nm.

3.5. Optical absorption

The optical absorption of PbS thin films was studied in the wavelength range 350 to 1050 nm. The variation of optical absorption α with wavelength λ is shown in Figure 8. All films show higher absorption on the shorter wavelength side. The nature of the transition (direct or indirect) is determined via the relation

$$\alpha = \frac{A\left(h\upsilon - E_g\right)^n}{h\upsilon} \tag{7}$$

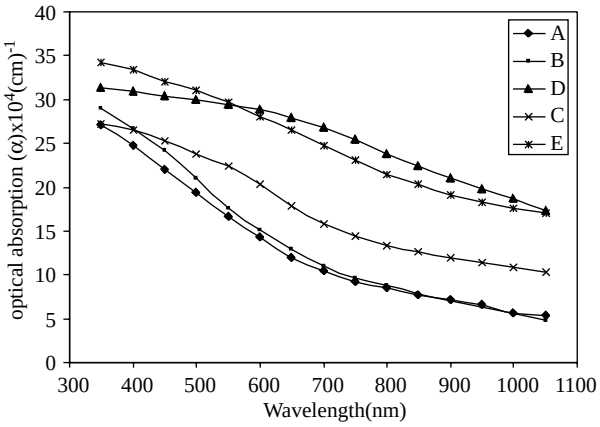

Figure 8. Plot of optical absorption vs. wavelength for PbS films with different thicknesses: (A) 65 nm (B) 98nm (C) 114 nm (D) 130 nm and (E) 168 nm.

where $h\nu$ is the photon energy E_g is the band gap energy, and A and n are constants. For allowed direct transitions $n = 1/2$; for allowed indirect transitions $n = 2$. The plots of $(\alpha h\nu)^2$ versus $h\nu$ are shown in Figure 9 for PbS films of various thicknesses. Variation of $(\alpha h\nu)^2$ with hν for PbS films is a straight line, indicating the presence of a direct transition. Band gap energy E_g was determined by extrapolating the straight-line portion to the energy axis for zero adsorption coefficient α. Figure 10 shows variation in optical band gap energy from 1.88 to 2.28 eV with thickness from 168 to 65 nm. This is attributed to the crystallite size-dependant properties of the energy band gap [18, 19].

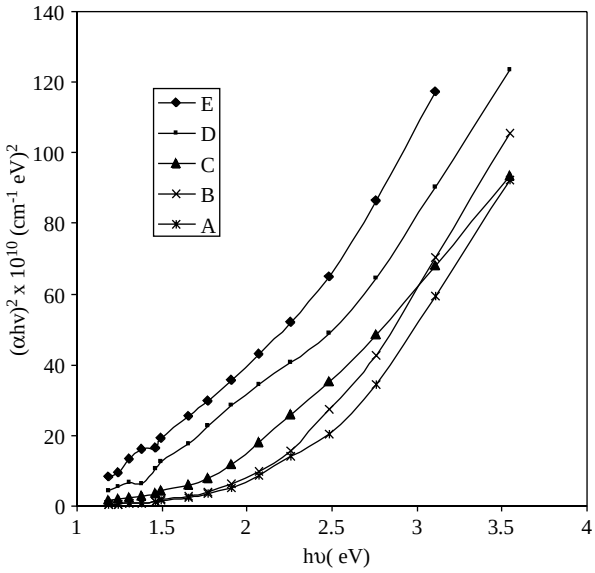

Figure 9. Plot of $(\alpha h\nu)^2$ versus $h\nu$ for PbS films with different thicknesses: (A) 65 nm, (B) 98 nm, (C) 114 nm, (D) 130 nm and (E) 168 nm.

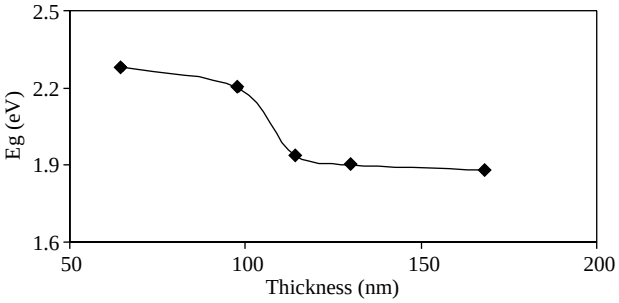

Figure 10. Variation of optical band gap energy E_g with film thickness.

4. Conclusions

Nanostructured PbS thin films at low temperature were prepared by a simple chemical Bath Deposition method. The results of XRD and SEM show that the deposited PbS film consists of nano-sized grains and the grain size increases with increasing film thickness. An XRD study shows nanocrystalline structure with cubic phase (galena). The Optical absorption study reveals that PbS thin films have allowed direct transitions. The optical band gap energy varies from 1.88 to 2.28 eV with thickness. The thermo-emf measurements confirm the p-type nature of PbS. The electrical resistivity and therefore activation energy are observed to be thickness dependent.

Acknowledgement

The authors are thankful to University Grants Commission, WRO, Pune (India), for financial support under the project (No: F47-15/2003). Also we would like to thank Prof. A. Mahajan of the Indian Institute of Technology, Mumbai (India), for the XRD measurements.

References

[1] L. E. Brus, *Appl. Phys.*, **53**, (1991), 465.

[2] A. Roy, A. Chainani, D. D. Sarma, and A. K. Sood, *Appl. Phys. Lett.*, **2**, (1989), 1779.

[3] Y. Wang and N. Herron, *J. Phys. Chem.*, **95**, (1991), 525.

[4] C. Weisbuch and B. Vinter, *Quantum Semiconductor Structures,* (Academic Press, New York. 1991).

[5] C. D. Lokhande, A. U. Ubale, and P. S. Patil, *Thin Solid Films*, **302**, (1997), 1.

[6] Y. Wang, A. Suna, W. Mahler and R. Kawoski, *J. Chem. Phys.*, **87**, (1987), 7315.

[7] N. I. Fainer, M. L. Kosinova, Yu. M. Rumyantsev, E. G. Salman and F. A. Kuznetsov, *Thin Solid Films*, **280**, (1996), 16.

[8] I. Pop, C.Nascu, V. Ionescu, E. Indrea and I. Bratu, *Thin Solid Films*, **307** , (1997), 240.

[9] R. Thielsch, R. Reiche, T. Bhome, D. Schlafer, H. D. Bauer and H. Bottcher, *Nanostruct. Matter.*, **10**, (1998), 131.

[10] C. Nascu, V. Vomir, I. Pop, V. Ionescu and R. Grecu, *Mater. Sci. Eng.,* **B841**, (1996), 235.

[11] S. B. Quadri, J. Yang, B. R. Ratna, F. E. Skelton and J. H. Hu, *Appl. Phys. Lett.*, **69**, (1996), 2205.

[12] T. P. Sharma, R. Kumar, G. Jain and S. C. K. Mishra, *Indian J. Pure & Appl. Phys.*, **29**, (1991), 583.

[13] V. Valenzuela-Jauregui, V. Ramirez-Bon, A. Mendoza-Galvan and M. Sotelo-Lerma, *Thin Solid Films,* **441**, (2003), 104.

[14] R. K. Joshi, A. Kanjilal and H. K. Seghal, *Appl. Surf. Sci.*, **221**, (2004), 43.

[15] K. K. Nanda and S. N. Shau, *Appl. Phys. Lett.*, **79**, (2001), 2743.

[16] S. Yang, S. Wang and K. K. Fung, *Pure Appl. Chem.*, **72**, 1, (2000), 119.

[17] K. M. Gadave, S. A. Jodgudri, and C. D. Lokhande, *Thin Solid Films*, **245**, (1994), 7.

[18] A. U. Ubale and D. K. Kulkarni, *Indian J. Pure. & Appl. Phys.*, **44**, (2006), 254.

[19] M. Y. Nadeem and Waqas Ahmed, *Turk. J. Phys.*, **24**, (2000), 651.